第 49 卷第 2 期
七月 2025

Diqiu Kexue - Zhongguo Dizhi Daxue Xuebao/Earth Science
Journal of China University of Geosciences

Vol. 50 No. 2
July - Dec 2025

DOI: 10.5281/zenodo.17851640

Numerical Investigation of the Effect of Soil-Structure Interaction on the Seismic Behavior of Steel Structures with Shear Walls

Sahira Mohsin Shaqi[a], Reza Moradi[b]

[a] MSc. in civil engineering, Ministry of Higher Education & Scientific Research, Scientific Research Commission, Baghdad, Iraq
[b] Ph.D. in civil engineering, adjunct professor, faculty of engineering of Eslamabad-e-Gharb, Razi University, Kermanshah, Iran

*Corresponding author: sahira.mohsin.shaqi@gmail.com

Published: 08 December 2025
Accepted: 21 November 2025
Received: 11 October 2025

Abstract: Generally, in the design of structures, the soil under the structures is considered rigid, and the effect of soil-structure interaction is ignored. However, the soil under the structure is not rigid in reality, and the presence of soil under the structure will cause changes in the dynamic characteristics of the structure and consequently change its response. The type of soil and the flexibility of the foundation are among the factors that can affect the analysis results to some extent. Therefore, depending on the type and depth of the soil of the construction site, building structures will have a different response to the bedrock. On the other hand, the effects of soil-structure interaction are due to inertial interaction and kinematic interaction. Of course, methods are proposed in some international seismic codes to analyze soil-structure interaction. However, due to the complexities of kinematic interaction, they often only consider the effects of inertial interaction. In this article, using Abaqus software, a three-dimensional model of a 5, 10, and 15-story steel structure with a core shear wall and side shear wall structural system is compared and investigated, taking into account various soil types under the structure and comparing it with a structure with a rigid foundation under earthquakes. The results of this research show that maximum shear forces at the base of a building are concentrated at the top surface of any rafts supported by hard shear walls, and they decrease upward. At the top of the raft, the bending moment reaches its maximum of 240%. In the shear-walls scenarios, bending moments and shear forces at the walls' base are significant regardless of the supporting soil media due to the connection with the raft foundation slab.

Keywords: *Soil-Structure Interaction, Period, Seismic Behavior, shear force, story drift*

1. Introduction

One of the most important factors affecting the determination of dynamic loads on a structure is the soil-foundation-structure interaction, which is very sensitive in the design and determination of dynamic parameters affecting it(Al Shamaa, Al Shimmeri, & Lazem, 2023; Arshadi, Kheyroddin, & Nezhad, 2022; Bharti, Garg, & Chandrawanshi, 2025; Ebadi & Farajloomanesh, 2020; Z. A. Hasan, Nasr, Kubba, & Hashim, 2025; Kheyroddin & Hemmati, 2020; Liu, Zhang, Li, Jin, & Zong, 2019; Maddahi, Gerami, & Naderpour, 2023; Mahdi, 2024; Mohammad, Fazel, & Reza, 2021; Najar et al., 2025; Nesterova, Uzdin, & Fedorova, 2018; Stastny, Emera, Galavi, & Tschuchnigg, 2025; Муаяд & Шашкин, 2023). Therefore, studying this issue as closely as possible and examining it specifically is one of the most important branches of earthquake engineering issues and seismic assessment of structures(Falah & Muteb, 2024; Forcellini, 2024; M. M. Hasan, Hore, Al Alim, Hore, & Ansary, 2025). It is obvious that determining the forces and stresses created in the structure under the influence of dynamic factors is one of the most important steps in structural analysis. Since these factors change greatly with the change in the mechanical conditions of the structure's foundation, as well as its dynamic parameters, the way the soil, foundation, and structure are related, and the type of function each of them performs in transferring forces and stresses from the soil to the foundation and then from the foundation to the structure and vice versa. Therefore, it is necessary that the condition of the soil under the foundation and around it and the structure, as well as the shape and amount of loads and stresses applied to it, as well as the changes in its mechanical parameters under the influence of these stresses and forces, be taken into account and carefully considered in the analyses. The effect of soil-structure interaction on creating stresses and forces in soil and structure is very large and sensitive and is influenced by many factors such as the degree of rigidity of the foundation and even the number of soil layers under the foundation, and the type of their arrangement(Bapir, Abrahamczyk, & Afroz, 2024; Katsimpini, 2024; Sun, Chen, Du, Huang, & Huang; Wrana, 2025). The reduction in the response of the structure is due to the scattering of waves from the foundation and the propagation of seismic energy of the structure into the soil. When the soil around the foundation experiences low to moderate nonlinear responses, the soil-structure interaction absorbs the energy of the vibration waves and therefore reduces the energy of the structure. The most important challenge in seismic design in the future is to accurately determine this amount of energy loss and include it in the design of the soil-structure system. More detailed research and further studies by researchers have shown that considering the soil-structure interaction increases the damping of the system and increases the effective period of the structure(Ali, Akhaveissy, & Abbas, 2024; Jasim & Al-Araji, 2025; Mohammed Ali, Besharat Ferdosi, Kareem Obeas, Khalid Ghalib, & Porbashiri, 2024; Mohammed Ali Al-Araji, Jasim, & Al-Kasob, 2025). In addition, this phenomenon causes the system to decrease or increase its response to incoming dynamic excitations, the amount of which depends on the dynamic parameters and characteristics of the structure. By considering the soil-structure interaction, the damping of the entire system can be divided into two dampings: the damping of the structure and the damping of the foundation. The damping of the structure is reduced by a factor that depends on the characteristics of the soil and the structure, but the damping of the foundation will increase the damping of the entire system. Previous studies have shown that the damping of the foundation is between zero and 25 percent.

2-Basic assumptions and numerical modeling method

2-1-Numerical models

Research was conducted on three structures: a fifteen-story building constructed of steel columns, beams, and concrete slabs; a ten-story building with the same materials; and a five-story building with the same materials. Each structure's raft is between 0.5 and 1.0 meters in thickness and measures 17.0 by 14.0 meters. Beam-column elements were successfully utilized in the modeling of the superstructure. It was assumed that each level would get a normal service loading of (8.0 kN/m2). The loads on the columns were placed at the four corners. The modulus of elasticity was calculated to be 24,870 MN/m2, and the self-weight was measured to be 24.0 kN/m3.

The floor plans (SW1, SW2, and SW3) and the three-dimensional model (Fig. 1) of a rectangular fifteen-story three-bay framed building on a raft base are presented, respectively. The components and specifications of the building are shown in Table 1. Solid elements connecting the column bases represent the raft foundation in the model. Beam-column elements stand in for the actual columns and beams in a construction. The column beam intersections are choke points

for the floor's mass. Cohesion and angle of internal friction for foundation soil modeled with C3D8R solid components and the Mohr-Coulomb failure criterion are given in Table 4-2. The beams and columns in the superstructure each have a 5% damping factor imposed on them at the element level.

Fig. (1) depicts a numerical model in three dimensions of a framed, fifteen-story skyscraper resting on a raft base. Here, unlike in the 2D model, the bulk of the floor is modeled in 3 dimensions. Each floor's diaphragm mass is assumed to be concentrated at its center of mass on the assumption that the diaphragms are rigid in plane. The displacements of the floor diaphragm as a rigid body are represented by the three degrees of freedom (two horizontal translations and torsional rotation) of the center of mass. The rigid diaphragm hypothesis does not limit the other three degrees of movement at the corresponding beam-column joints.

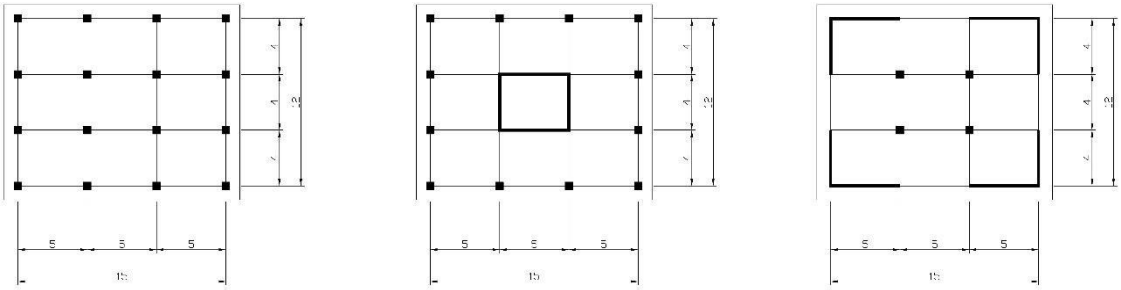

Figure (1): *floor plan of structures in this paper*

Table (1): *Summary of dimensions of structural elements (m)*

Structures	Stories	Columns	Beams	Shear walls	Slabs
5-storey	1 ~ 3	Box 400 x 12	IPE 300	NA	0.15
	4 ~ 5	Box 350 x 10	IPE 300	NA	0.15
10-storey	1 ~ 3	Box 450 x 15	IPE 300	NA	0.15
	4 ~ 6	Box 400 x 12	IPE 300	NA	0.15
	7 ~ 10	Box 350 x 10	IPE 300	NA	0.15
15-storey	1 ~ 3	Box 550 x 20	IPE 300	200	0.15
	4 ~ 6	Box 500 x 18	IPE 300	200	0.15
	7 ~ 9	Box 450 x 15	IPE 300	200	0.15
	10 ~ 12	Box 400 x 12	IPE 300	200	0.15
	13 ~ 15	Box 350 x 10	IPE 300	200	0.15

2-2-Earthquake characteristics

Ground motions caused by earthquakes vary in terms of location-specific factors, magnitude, and frequency content. The input time series are derived from actual records of five separate earthquakes. Table (2) details the various earthquake records that were considered. Base shear ratio (the horizontal base shear force divided by the total weight of the superstructure) is kept below 0.3 by using a subset of each earthquake record in this analysis. For these loads, it is anticipated that the superstructure will retain its elasticity.

Table (2): *List of Earthquake Motion and Parameters of Seismic Records*

Earthquake	Country	Year	PGA (g)	Moment magnitud (R)	Duration (s)	Type	Hypocentra distance (km)
El-Centro	USA	1940	0.349	6.9	56.5	Far field	15.69
Hachinohe	Japan	1968	0.229	7.5	36.0	Far field	14.1
Kobe	Japan	1995	0.833	6.8	50.0	Near field	7.4
Northridge	USA	1994	0.843	6.7	30.0	Near field	9.2
San Fernando	USA	1971	1.075	6.4	42.0	Near field	8.1

The amount of earthquake force exerted on a building is typically represented as a fraction of the official maximum. El Centro has 35% of the records, Taft has 75%, Loma Prieta has 40%, Northridge has 25%, and San Fernando (Pacoima Dam) has 25%.

2-3- FEM Modelling

A wide range of elements representing various structural components can be found in the Abaqus collection. Beams, columns, floor slabs, and the raft foundation are modeled in this investigation using three-dimensional (3D) beam elements (B31) and four-dimensional (4D) elastic shell elements (S4R). In order to incorporate the structure's underlying character, two distinct sorts of elements are used. Two types of elements are used to model the infinite soil (elastic continuum) below a building: the structural mass element, which groups structural masses at nodal locations, and the three-dimensional, eight-node reduced integrating element C3D8R. Below is a comprehensive breakdown of each component(Al Araji, Moradi, & Owaid, 2025; Khalilzadehvahidi & Moradi, 2019; Moradi & Khalilzadeh Vahidi, 2018, 2021; Moradi & Khalilzadeh, 2021; Vahidi & Moradi, 2019).

Damping coefficients (and) are calculated using the first and second natural frequencies of the structure, with a damping ratio of 5% assumed (Van Nguyen et al., 2017). Additionally, yield stress is defined, and elastic-perfectly plastic behavior is applied to structural parts.

The beam element used is elastic, uniaxial, three-dimensional, and may undergo tension, compression, torsion, and bending. The element is bi-nodal, with six degrees of freedom per node (X, Y, and Z translations, and rotations about the nodal axis). When developing the structural model of the frame structure, this element stands in for the columns and beams of the superstructure as well as the beam-column elements of the raft.

The floor slabs were designed using an elastic shell element. These elements are susceptible to membrane stresses as well as bending forces. Each node has six degrees of freedom. The element is characterized by the uniform thickness and bidirectional orthotropic characteristic material qualities at each of its four nodes. The shell parts in the building model are flattened out to zero curvature to simulate a flat floor.

A lumped mass element is used to model the structural elements' masses as well as the dead loads acting upon them. Here we use it for concrete floor mass substitution and applied floor superimposed loading.

The Mohr-Coulomb failure criterion is used in conjunction with the C3D8R solid element model to simulate the soil component. The table (3) below details the cohesion and friction angle and tension cut-off choice needed to do this in Abaqus.

Table (3): *Soil Types and Input Parameters (Elastic Continuum Model).*

Soil Type	Shear wave m/sec	Soil Class	Soil Modulus KPa	Poisson's ratio	Soil Density Kg/m^3	Cu KPa	Friction Angle
I	450	GM	69,000	0.40	1730	0	40
II	320	CL	15,600	0.45	1730	24	19
III	150	CL	7,500	0.50	1470	20	10

Sun et al. (1998) and Seed et al. (1986)'s cyclic shear strain (c) depended shear modulus ratio(G/Gmax) and damping ratio (ζ) curves are adopted for clayey soils (A and B soil) and sandy soils (C soil), respectively, to account for the nonlinearity of subsoil. The strain-compatible ratios for damping, shear modulus of the soil under seismic events (Table 3) were then determined by trial and error. Both Fatahi and Tabat-abaiefar (2014) and Tabat-abaiefar et al. (2013) provide in-depth descriptions of each stage of this procedure.

The energy dissipation in the soil during an earthquake is accounted for using the Rayleigh damping model. Choosing soil frequencies is crucial since they establish the and damping coefficients. Park and Hashash (2004) proposed a methodology for selecting soil frequencies so that they would at least partially cover the primary frequency spectrum of the seismic record; this is the approach taken in the present investigation.

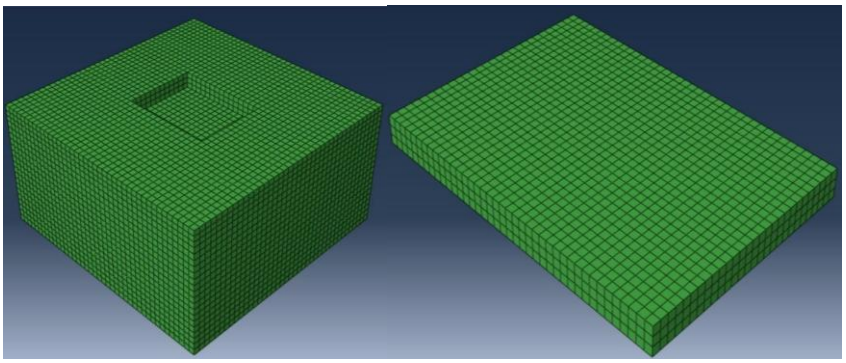

(a) (b)

Figure (2): *Three-dimensional solid (a) soil element (C3D8R) (b) raft element (C3D8R)*

Abaqus's surface-to-surface contact standard element was used to model and simulate the raft foundation's interaction with the surrounding elastic continuum (soil) under applied loadings. The bottom side of the concrete raft serves as the system's master surface, while the top of the earth acts as its slave. This is because the mesh dimensions of these two surfaces are comparable, and the foundation is made of a stiffer material. There are also surface-to-surface discretization and finite-sliding formulations used.

The accuracy of the dynamic analysis has been checked using ABAQUS. The type of dynamic analysis used in this

investigation has a number of potential implementations. Among these are spectral analysis, transient dynamic analysis, and modal analysis. For the time-history analysis, we use transient dynamic analysis. Each case study's modal analysis yields the frequency ranges and periods of the various mode shapes.

3-Results and Discussion

3-1-Type of soil stiffness and Raft flexural rigidity parameter

Fig. (3) shows the variations in total settlements in the raft for different types of soils (I, II, and III) shown on the bottom axis as (1, 2, and 3). And different lateral movement structural resisting systems (with shear-walls sw1, sw2, and without shear-walls Moment Resisting Frame, sw3). The three values of the modulus of subgrade reaction correspond to soft, medium, and stiff soils, Table 5-1. The settlement comes down with an increase in soil stiffness. Similar to how total settlements decrease with increasing soil stiffness, differential settlements do so as well. However, there is little variation in the raft's maximum bending moments, but the raft's values are typically greater for stiffer soils towards its margins.

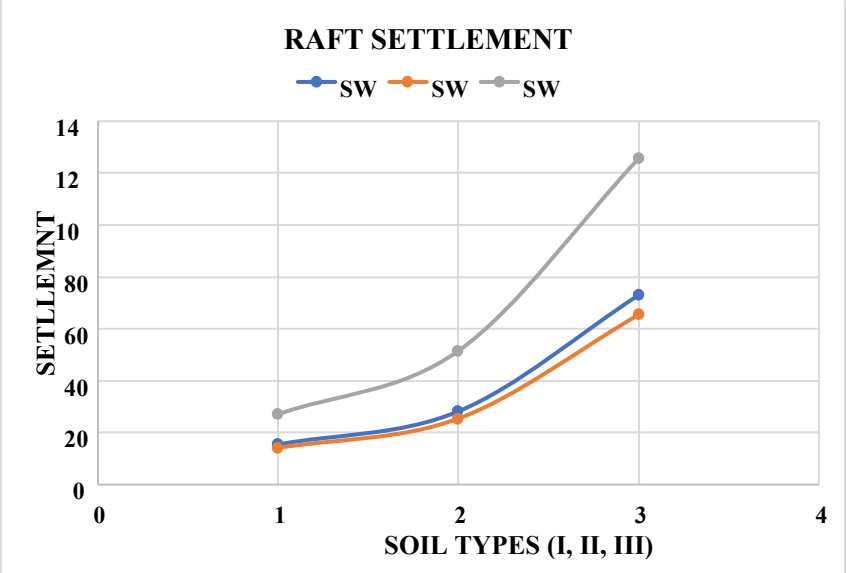

Figure (3): *Soil Settlements for each structural lateral resisting system and soil types.*

To investigate the impact of superstructure stiffness on maximum settlements in the raft, the preceding building model is investigated both with and without considering the superstructure lateral resisting systems (shear-walls) above the raft. Figure (3) displays quantitative comparisons of the mat's total settlements. The building follows the same pattern in both shear-wall structural system cases, as shown in the pictures below. When the shear-walls structural system is considered, the settlement values decrease, and the maximum bending moment in the raft increases significantly.

The structural performance of the building's concrete base is investigated when its raft thickness varies from 0.5 to 0.75 to 1.0 meters. Figure (4) displays the outcomes of the analyses that ignore the superstructure. It is seen that the flexibility of the foundation does not significantly affect the overall settlement. Variations in raft thickness are found to have a major impact on the differential settlements. The maximum bending moments also vary among the three scenarios.

A comparison of the two sets of figures (with and without the shear-walls structural system) reveals striking differences in the outcomes for the raft with and without the shear-walls structural system. However, when the shear-walls system is taken into account, the settlement values (both total and differential) are slightly lower, and the raft moments are significantly larger.

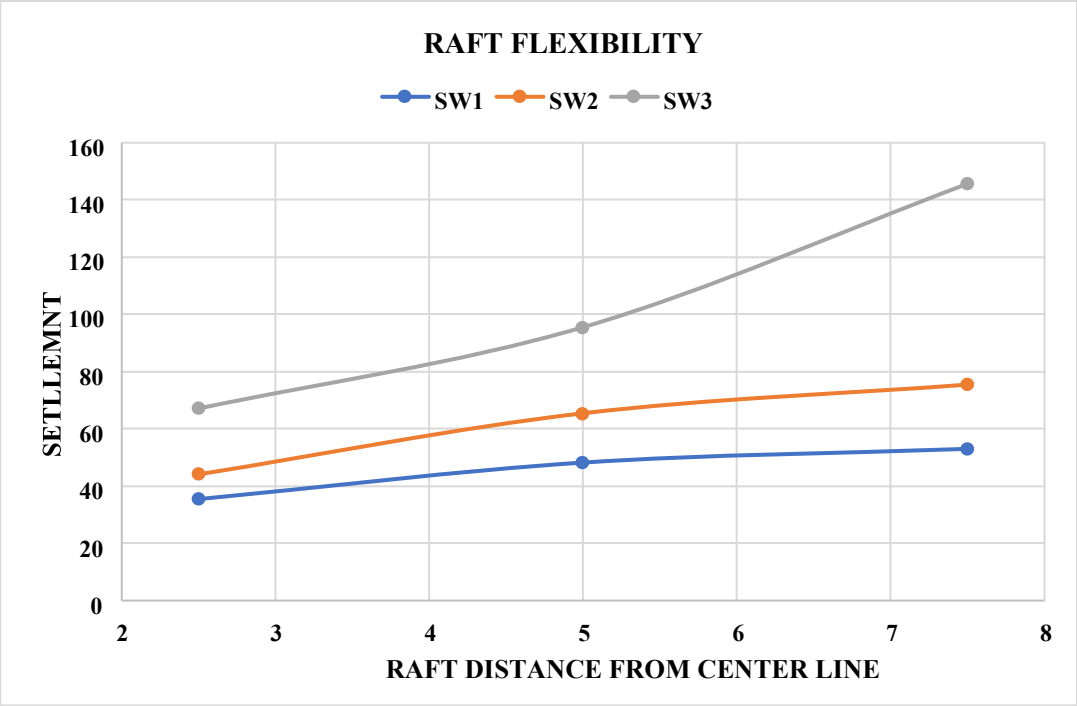

Figure (4): *Effect of foundation flexural rigidity on total settlement considering the shear-walls structural systems effects.*

3-2- Seismic response of tall buildings considering soil-structure interactions

Soil-structure interaction is typically disregarded in traditional seismic design of buildings. Since soil-structure interaction typically reduces structural reaction, assuming structures have a fixed foundation leads to conservative results. The effect is conditional on a number of factors, such as the soil's stiffness and damping, the nature of the ground motion, and the structure's features. However, there is no straightforward way to quantify the consequences. Although simplified analysis approaches for soil-structure interaction have been presented, it is necessary to investigate whether they apply to a wide range of building configurations and earthquake characteristics. The results of this investigation are analyzed using three-dimensional numerical models. We examine the effects of various building and foundation characteristics on five-, ten-, and fifteen-story raft-supported buildings.

3-3- The phenomenon of soil and structure interaction in dynamic systems

The structural response of a building can be affected in two different ways by the soil-structure interaction. The ground beneath a structure can be distorted by the inertial forces created by an earthquake. Soil horizontal displacement is caused by horizontal base shear in the building columns, and rocking motion in a tall building is caused by moment about the base due to inertia forces. Fundamental period elongation happens when horizontal soil flexibility is present. Waves that go through the ground also disperse their energy there.

When considering structural response, these two impacts are almost always positive. On the other hand, greater shear pressures are a direct result of the increased acceleration of building masses caused by the swaying motion of high-rise structures due to soil flexibility.

3-4-Time-history analysis

The El-Centro earthquake is also applied in this parametric study that uses the same building design parameters. The

building floor systems were considered as a mass-lumped to its geometric nodes. It is assumed that the building and soil parameters, as well as the columns and beams section, are the same as those in Sec 5.4 that concern 3D FEM analysis. Time-history analysis in Abaqus was performed using this framework. On top of that, ABAQUS uses modal analysis to identify the structure's inherent resonant frequencies, periodical modes, and mode shapes.

In order to find out the impact of various factors, three-dimensional models (of 5, 10, and 15 stories) are tested with different soil types (Soil I, II, and III), building characteristics, and recorded ground motion. In what follows, we'll look at the results for each one individually. Maximum column base shear and maximum building drift are the primary parameters used to characterize the reactions of buildings. Maximum base shear is defined as the maximum relative displacement between the top and the ground floor, while maximum building drift is defined as the maximum total horizontal shear pressures in all the columns at the ground floor level. These numbers represent the stresses on the elements and the system's deformation, respectively.

3-5-Type of soil and soil stiffness parameter

The stiffness of the earth beneath a building is the single most critical factor. It provides some insight into the nature of the underlying geological media. This research classifies soils according to the shear wave velocities that propagate across them.

Let's start with a look at the three-bay building's digital prototype in three dimensions (Fig. 5-15). These numbers show that when soil stiffness rises, so does the base shear coefficient. So, soil flexibility leads to a lower base shear coefficient. We can conclude that the structural reaction is diminished when soil-structure interaction is taken into account. This is especially the case for soft soils, where shear wave velocities are rather low. Base shear can be reduced by as much as 70%, 12%, and 14% due to soil-structure interaction. For more robust soils, however, the impact may be negligible. Shear values at the base (10 and 15 stories) are found to be quite close to those predicted by a stiff soil and rigid-base model. The Taft earthquake, however, demonstrates that base shear can grow when soil stiffness decreases.

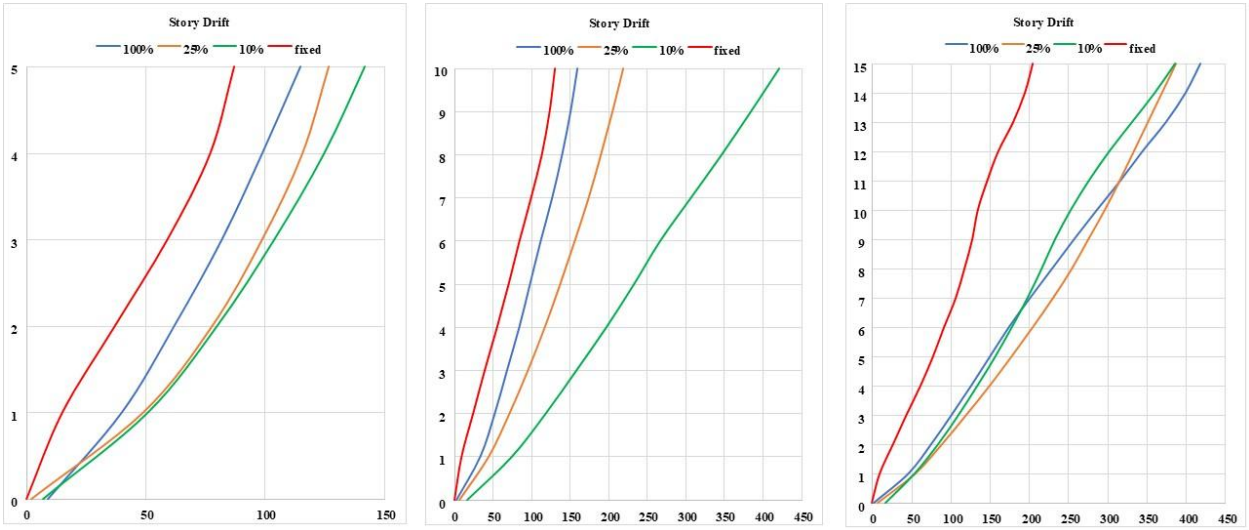

(a) (b) (c)

Figure (5): *Building Story drifts in z-direction 3D analysis of (a) 5-story, (b) 10-story, (c) 15-story for different soil conditions.*

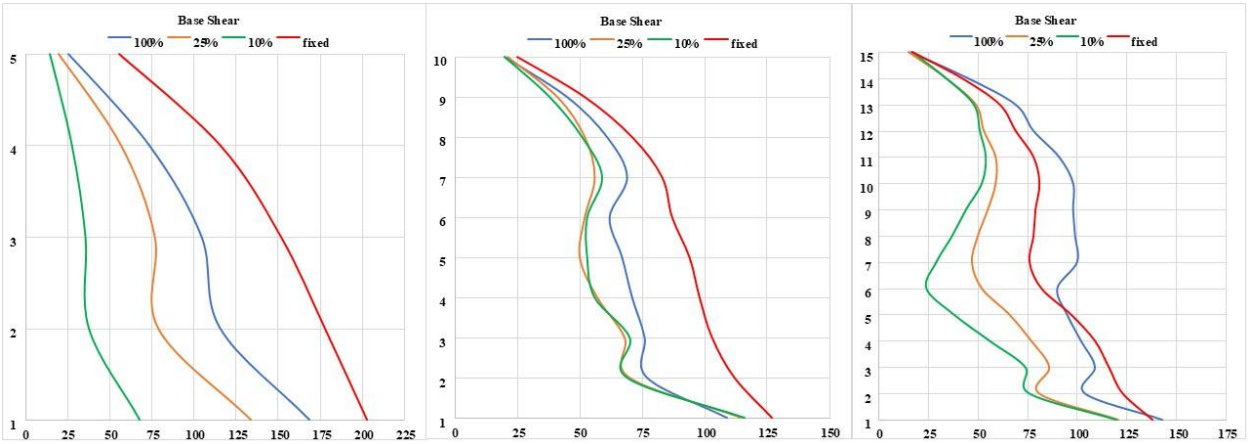

(a) (b) (c)

Figure (6): *Building Column base shear in z-direction 3D analysis of (a) 5-story, (b) 10-story, (c) 15-story for different soil conditions.*

3-6-Lateral resisting structural system parameter

Maximum lateral deformations of 5-, 10-, and 15-story buildings in stiff, medium, and soft soils, respectively, under the impact of El-Centro earthquake records, are depicted in Figures (7). Maximum lateral deformations of flexible-base structures have been increased in comparison to their rigid-base counterparts across the board regarding height, raft foundation thickness, and soil types. This is because the displacement response spectrum curve normally rises with an increase in the natural period of the system, and the degree of freedom of the soil-structure system rises after taking SSI into account. High-rise structures' displacement responses were amplified as a result.

However, the variation of displacement response of the classical rigid-base structures is relatively dramatic, especially when subjected to the action of wide-amplitude earthquakes, even when the lateral resisting structural system parameters are strong (along all levels of the building). Therefore, buildings supported on a raft foundation are more likely to be damaged by variations in soil quality.

Complex relationships exist between the maximum lateral story drift and the Building height-width ratio (H/B = 3.75, 2.5, and 1.25). Buildings' stability and resistance to the rotation of their foundations can both benefit from wider footprints. However, as building widths expand, their masses grow, leading to greater gravitational force and distortions in structure during earthquakes. Therefore, as the height-to-width ratio varies, so does the maximum lateral story-drift. In this case, the proportions were very close (/H = 7.4, 7.5, 8.0).

3-7-Building structural height parameter

When figuring out how flexible the building's superstructure will be, the height of the building is a vital consideration to take into account. This research takes into consideration the height of buildings from 5 to 15 stories.
As the height of the building is increased, we can observe from Figs. (8 to 9) that the range of base shear ratios decreases until it reaches a minimum. As a result, the structure will have more adaptability as additional levels are added. The results of a five, ten, and fifteen-story building were plotted independently for the EI-Centro earthquake in the following order: 8.0, 7.5, and 7.0, respectively. This was done so that you could get a better picture.

3-8-Building torsional rigidity parameter

As shown in Figure 5-22, the mass of a building with a symmetrical floor plan is altered by utilizing a variety of shear-wall systems at each floor level to conduct research into the influence of torsion on the structure. When seismic motion is applied to this model for different soil conditions, we observe that the base shears grow with increased soil flexibility, which is a pattern that is analogous to the symmetric mass building. The values of the base shears, on the other hand, are slightly greater than the symmetrical mass condition. As a result of the incorporation of torsional shear into the structure, this is completely understandable. The comparison results of building story drifts for the three structural systems under the El-Centro seismic excitation loadings are shown in Fig. (7 and 8)

There is a certain shear occurring in the transverse plane of the building as a result of the torsional impacts. These are quite a bit less than the values that correspond to those in the major direction. However, it is important to note that they also follow the same tendency of growing for stiffer soils, just like those that move in the other direction. For the El Centro earthquake, the base shear rate in this direction is always low, which is the case for the fixed base.
Additionally observable are the rotational motions at the top story that result from the torsional motion. According to the findings, the value of the rotation grows as the stiffness of the soil does as well. Torsional rotation of the topmost floor is approximately 0.15 degrees for a stiff foundation condition during the EI-Centro earthquake; however, it is always less than that with a flexible soil state due to the earthquake.

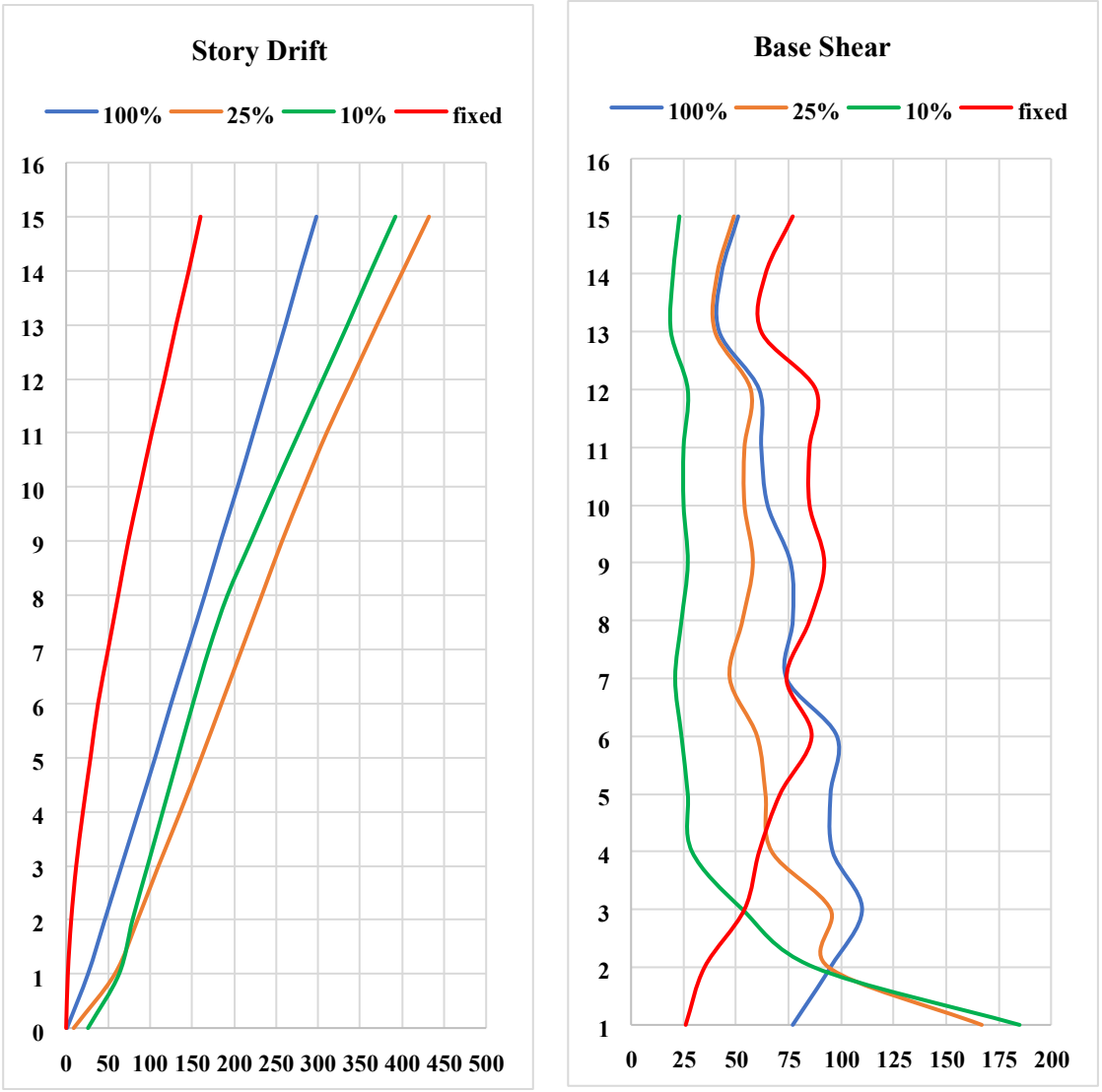

Figure (7): *Comparison between the results with Interior core shear-walls for different soil types.*

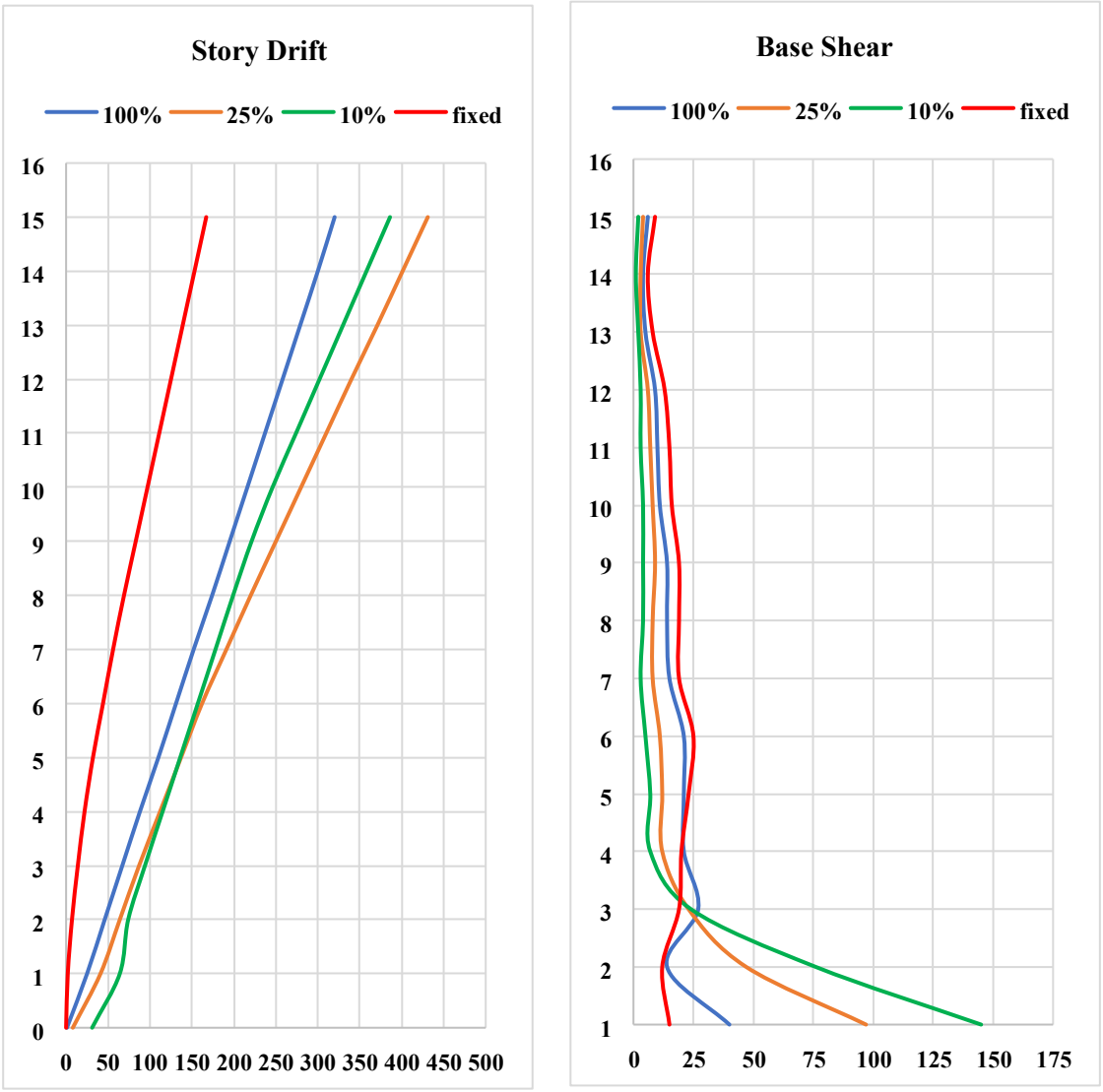

Figure (8): *Comparison between the results with Exterior angular shear-walls for different soil types.*

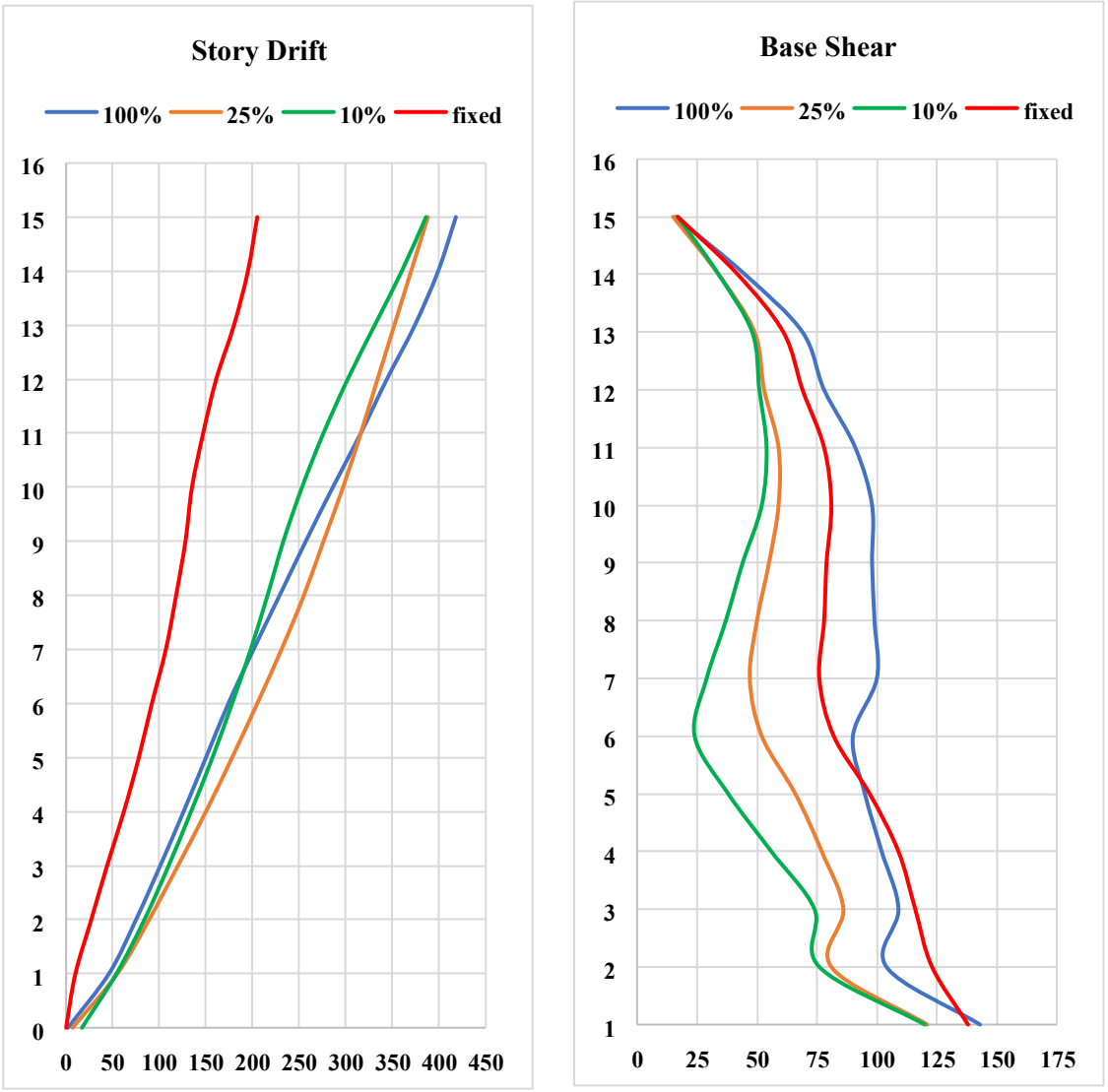

Figure (9): *Comparison between the results without shear-walls (MRF) for different soil types.*

4-conclusion

Soil-raft-structure systems with various foundations were analyzed in three dimensions with seismic loads. Several methods of lateral resistance were studied. The soil behavior was modeled using the linear elastic completely plastic constitutive model and the Mohr-Coulomb failure criterion. The dynamic properties of the superstructure's influence on the reaction of the systems were studied by implementing structures with 5, 10, and 15 stories.

The computations yielded both qualitative and quantitative information of interest concerning the foundations and the building's responses. Given the constraints of the accepted modeling and the enforced circumstances, the following conclusions can be drawn from the numerical results and applied to other engineering projects. It should be noted that experimental research is required to fully confirm the reported numerical results.

1- Building columns supported by shear walls and a raft foundation experienced lower base shear stresses than those without shear walls. This is because the torsional and lateral rigidity of the structure has been increased due to the fixed connection at the column heads and diaphragm slabs.

2- Buildings with 10 and 15 stories have SSI base shear forces that are lower than those of the 5-story instance, and the same is true for the raft and rigid shear-walls inclusion systems.

3- In contrast to the 5-story structure, the fundamental period of the systems with the 10- and 15-story buildings occurs in a region of the response spectrum where the acceleration is greater (closer to the resonance).

4- Strong lateral resisting systems cause significantly less swaying in buildings compared to those without such a system. When compression pressures operate on one side of the raft foundation, settlement values are reduced because of the contact with the bottom supporting soil medium.

5- When the SSI is taken into account, lateral displacements and tale drifts are magnified in comparison to the fixed-base situation. Rigid external shear-wall inclusion systems with a 5-story building always have the least maximum lateral displacement at the top node level compared to any other type of shear-wall.

6- The maximum shear forces in the column systems are higher in the systems with the 5-story structure (without shear-walls) than in the systems with the rigid shear-walls included. This growth is caused by the tremendous lateral stresses acting on the columns where they join the raft base.

7- Maximum shear forces at the base of a building are concentrated at the top surface of any rafts supported by hard shear walls, and they decrease upward. At the top of the raft, the bending moment reaches its maximum of 240%. In the shear-walls scenarios, bending moments and shear forces at the walls' base are significant regardless of the supporting soil media due to the connection with the raft foundation slab.

8- All building forces can be decreased by using the stiff shear-walls inclusion technique. It's useful in earthquake-prone regions with thin soil layers.

9- In contrast to the angular shear-wall and outside building side examples, the moments and shear forces at the raft top-surface are greater for the core shear-wall system. This is because there are more kinematic ground forces concentrated in the raft's core region. In order to prevent foundation failures at this stress concentration zone, this must be taken into account during the construction of the rigid shear-wall system.

References:

Al Araji, A. M., Moradi, R., & Owaid, A. M. (2025). Numerical investigation of bearing capacity and lateral response of pile group considering soil interaction. *Salud, Ciencia y Tecnología-Serie de Conferencias, 4*, 1582.

Al Shamaa, M., Al Shimmeri, A. J. H., & Lazem, A. (2023). Lateral bracing and steel shear wall integration in steel high-rises. *Magazine of Civil Engineering, 123*(7), 105-117.

Ali, A. M., Akhaveissy, A. H., & Abbas, B. (2024). Fire Behavior of Lightweight Reinforced Concrete Deep Beams and Enhanced Structural Performance via Varied Stirrup Spacing–An Integrated Study. *Journal of Rehabilitation in Civil Engineering, 12*(3), 132-151.

Arshadi, H., Kheyroddin, A., & Nezhad, A. A. (2022). High-strength steel effects on the behavior of special shear walls. *Magazine of Civil Engineering, 111*(3), 11102.

Bapir, B., Abrahamczyk, L., & Afroz, A. (2024). *Evaluation of Soil-Structure Interaction for Different RC Structural Systems and Foundation Sizes.* Paper presented at the Journal of Physics: Conference Series.

Bharti, A. K., Garg, V., & Chandrawanshi, S. (2025). *A critical review of seismic soil-structure interaction analysis.* Paper presented at the Structures.

Ebadi, P., & Farajloomanesh, S. (2020). Seismic design philosophy of special steel plate shear walls. *Magazine of Civil Engineering*(3 (95)), 3-18.

Falah, M. W., & Muteb, H. H. (2024). Open engineering: Evaluation of mechanically stabilized earth retaining walls for different soil–structure interaction methods: A review.

Forcellini, D. (2024). *A 3-DOF system for preliminary assessments of the interaction between base isolation (BI) technique and soil structure interaction (SSI) effects for low-rise buildings.* Paper presented at the Structures.

Hasan, M. M., Hore, S., Al Alim, M., Hore, R., & Ansary, M. A. (2025). Numerical modeling of seismic soil-pile-structure interaction (SSPSI) effects on tall buildings with pile mat foundation. *Arabian Journal of Geosciences, 18*(1), 10.

Hasan, Z. A., Nasr, M. S., Kubba, H. Z., & Hashim, T. M. (2025). Early and long-term performance of green mortar made from the waste of electrical cables. *Magazine of Civil Engineering, 18*(4), 1.

Jasim, M. H., & Al-Araji, A. M. A. (2025). Low speed impact on sandwich beam with flexible core and face sheets reinforced with FG-CNTs. *World Journal of Engineering, 22*(1), 141-147.

Katsimpini, P. S. (2024). Seismic Response of Vertical Hybrid Concrete/Steel Frames Considering Soil–Structure Interaction. *Buildings, 14*(4), 972.

Khalilzadehvahidi, E., & Moradi, R. (2019). Performance Pathology of Historic Adobe Structures and Their Methods of Retrofitting.

Kheyroddin, A., & Hemmati, A. (2020). Seismic behavior of end walls in RC tall buildings with torsional irregularity. *Magazine of Civil Engineering*(5 (97)), 9707.

Liu, Z.-Q., Zhang, J., Li, F., Jin, H.-P., & Zong, Z.-Y. (2019). An improved membrane element for high-rise building with shear walls. *Magazine of Civil Engineering*(7 (91)), 121-128.

Maddahi, M., Gerami, M., & Naderpour, H. (2023). Effect of uncertainties of shear wall on reliability of rehabilitated structure. *Magazine of Civil Engineering, 117*(1), 11701.

Mahdi, K. (2024). Performance of geosynthetics-strengthened unconnected piled raft foundations under seismic loading. *Magazine of Civil Engineering, 17*(3), 12704.

Mohammad, H., Fazel, A., & Reza, G. A. A. (2021). Numerical investigation of truss-shaped braces in eccentrically braced steel frames. *Magazine of Civil Engineering*(2 (102)), 10208.

Mohammed Ali, A., Besharat Ferdosi, S., Kareem Obeas, L., Khalid Ghalib, A., & Porbashiri, M. (2024). Numerical study of the effect of transverse reinforcement on compressive strength and load-bearing capacity of elliptical CFDST columns. *Journal of Rehabilitation in Civil Engineering, 12*(1), 106-126.

Mohammed Ali Al-Araji, A., Jasim, M. H., & Al-Kasob, B. D. H. (2025). LVI analysis on the beams with nonuniform cross-sectional area using exponential shear–strain function. *World Journal of Engineering, 22*(4), 876-880.

Moradi, R., & Khalilzadeh Vahidi, E. (2018). Comparison of numerical techniques of masonry infilled rc frames for lateral loads. *Journal of Concrete Structures and Materials, 3*(2), 102-118.

Moradi, R., & Khalilzadeh Vahidi, E. (2021). Experimental study of rotational-friction damper with two slip load and evaluation of its performance in RC frame under cyclic loading. *Journal of Concrete Structures and Materials, 6*(1), 121-137.

Moradi, R., & Khalilzadeh, V. E. (2021). General study of new ideas and practical of friction dampers for passive vibration control

of structures.
Najar, I. A., Ahmadi, R., Amuda, A. G., Mourad, R., Bendary, N. E., Ismail, I., . . . Tang, S. (2025). Advancing soil-structure interaction (SSI): A comprehensive review of current practices, challenges, and future directions. *Journal of Infrastructure Preservation and Resilience, 6*(1), 5.
Nesterova, O., Uzdin, A., & Fedorova, M. Y. (2018). Method for calculating strongly damped systems with non-proportional damping. *Magazine of Civil Engineering*(5 (81)), 64-72.
Stastny, A., Emera, A., Galavi, V., & Tschuchnigg, F. (2025). Cyclic soil-structure interaction of integral railway bridges. *Frontiers in Built Environment, 11*, 1541282.
Sun, W., Chen, Y., Du, Q., Huang, Z., & Huang, L. Physics-guided deep learning-based constitutive modeling for the gravelly soil-structure interface. *Zia and Huang, Linchong, Physics-Guided Deep Learning-Based Constitutive Modeling for the Gravelly Soil-Structure Interface*.
Vahidi, E. K., & Moradi, R. (2019). Numerical study of the force transfer mechanism and seismic behavior of masonry infilled RC frames with windows opening. *Civil Engineering Journal, 5*(1), 61-73.
Wrana, B. (2025). Nonlinear elastic-plastic model of soil-structure interaction in time domain. *WIT Transactions on The Built Environment, 3*.
Муаяд, С. М., & Шашкин, К. Г. (2023). Soil-structure interaction: theoretical research, in-situ observations, and practical applications. *Magazine of Civil Engineering, 120*(4), 12005.


creative
commons